

On distinguishing age from metallicity with photometric data

Baitian Tang^{1*} and Guy Worthey^{1†}

¹*Department of Physics and Astronomy, Washington State University, Pullman, WA 99163-2814, USA*

Accepted . Received ; in original form 2011

ABSTRACT

In the study of galaxy integrated light, if photometric indicators could extract age and metallicity information of high enough quality, photometry might be vastly more efficient than spectroscopy for the same astrophysical goals. Toward this end, we search three photometric systems: David Dunlap Observatory (DDO), Beijing-Arizona-Taiwan-Connecticut (BATC), and Strömrgren systems for their ability to disentangle age and abundance effects. Only the Strömrgren $[c_1]$ vs. $[m_1]$ plot shows moderate age-metallicity disentanglement. We also add to the discussion of optical to near-infrared Johnson-Cousins broad band colours, finding a great decrease in age sensitivity when updated isochrones are used.

Key words: galaxies: abundances — galaxies: evolution — galaxies: general — galaxies: photometry — galaxies: stellar content

1 INTRODUCTION

Since the concept of stellar populations was invented (Baade 1944), stellar population synthesis (SPS) has been proven to be a useful tool for revealing clues about galaxy formation (Tinsley 1968, 1978; Bruzual & Charlot 1993). Research on several crucial factors of stellar modelling, like convection, opacity, heavy-element mixing, helium content, and mass loss (Charlot et al. 1996), resulted in increasingly accurate SPS models (Bruzual & Charlot 1993; Worthey 1994; Bertelli et al. 1994; Bruzual & Charlot 2003; Dotter et al. 2008; Bertelli et al. 2008, 2009). In this scheme, estimation of single burst equivalent age and metallicity, was accomplished by comparing integrated light of observed galaxy with that of SPS models. However, most of the colours and absorption feature strength appear identical if the changes of age and metallicity satisfy $\delta \log(\text{age}) \approx -3/2 \delta \log(Z)$. This so-called age-metallicity degeneracy (Worthey 1994) blocks the way to estimating galaxy accurate ages from optical broad band colours. At spectroscopically narrow bands, however, several age sensitive or metallicity sensitive Lick indices (Burstein et al. 1984; Faber et al. 1985; Gorgas et al. 1993; Worthey et al. 1994; Worthey & Ottaviani 1997; Thomas et al. 2003), taken in pairs, are effective at breaking this degeneracy. Balmer indices vs. Fe-peak indices are widely used, for example, because they are relatively easy to observe (all features are

in the optical so one spectrograph can cover them all) and the model grids in the observed index-index space open up to nearly orthogonal grids rather than collapsed into linear, degenerate overlapping segments.

Spectroscopy is effective, but photometry also has its strong points. It is much more efficient for faint objects and low surface brightness galaxies. In the epoch of large sky surveys, like *Sloan Digital Sky Survey (SDSS)*, *Two Micron All Sky Survey (2MASS)*, *Spitzer Space Telescope (SST)*, *Large Synoptic Survey Telescope (LSST)*, and *James Webb Space Telescope (JWST)*, photometry is undoubtedly more feasible than spectrometry. In fact, optical near-infrared (near-IR) colours have been exploited to possibly constrain age and metallicity by several studies (Peletier et al. 1990; de Jong 1996; Bell & de Jong 2000; Carter et al. 2009; Conroy et al. 2009). Cardiel et al. (2003) suggested ($V - K$) colour shows good balance between parameter degeneracy and sensitivity. Pessev et al. (2008) found that four age intervals (>10 Gyr, 2–9 Gyr, 1–2 Gyr, and 0.2–1 Gyr) are clearly separated in the optical near-IR colour-colour plot. These results hinge upon the models, and specifically upon the number of thermally pulsing asymptotic giant branch (TP-AGB) stars, which dominate near-IR light between 0.3 and 2 Gyr of age (Maraston 2005; Lee et al. 2007).

The present work looks for age-sensitive or metallicity-sensitive indices in three photometric systems: David Dunlap Observatory (DDO, McClure & Van den Bergh 1968; McClure 1976), Beijing-Arizona-Taiwan-Connecticut (BATC, Fan et al. 1996; Shang et al. 1998), and Strömrgren (Strömrgren 1966; Rakos et al. 1991, 1996) systems. These

* E-mail: baitian.tang@email.wsu.edu (BT)

† E-mail: gworthey@wsu.edu (GW)

Table 1. Metallicity sensitivities at 8 Gyr, solar metallicity, for our best candidate pairs of colors

Index	Z_{sp}
DDO C(41-42)	-0.60
DDO C(35-48)	1.42
BATC 6075-6660	1.15
BATC 5795-6075	1.97
Strömgren [m_1]	1.23
Strömgren [c_1]	2.41

filters are narrower in wavelength than Johnson-Cousins broad band filters, but resemble the *NIRCam* narrow filters¹ on board *JWST*. Can we find indices which are practical to break the age-metallicity degeneracy? The tables and graphs in § 2.1 explore this issue. In addition, equipped with the latest stellar evolutionary isochrones of the Padova group² (Bertelli et al. 2008, 2009, hereafter B09), we plot the model grids in $(B - V)$ vs. $(V - K)$ space, and compare with previous models in § 2.3. Observables from three samples are chosen to verify the credibility of parameters given by the model grids. Discrepancies between two model grids are briefly discussed in § 3, and a brief summary of the results and outlook for the future is given in § 4.

2 ANALYSIS

2.1 DDO, BATC & Strömgren

In order to find the age-sensitive or metallicity-sensitive index, we calculate the the metallicity-to-age sensitivity parameter (Z_{sp}) using the evolving Worthey (1994, hereafter W94) models, following Worthey (1994) and Serven et al. (2011). The spectral library is synthetic and is sensitive to individual elemental abundances in the 300 to 1000 nm wavelength range. The metallicity sensitivity parameter is:

$$Z_{sp} = \frac{\delta I_m / \delta \log(Z)}{\delta I_a / \delta \log(\text{age})} \quad (1)$$

Where $\delta I_m / \delta \log(Z)$ is the metallicity partial derivative of the index at 8 Gyr, and $\delta I_a / \delta \log(\text{age})$ is the age partial derivative of the index at solar metallicity. Thus, Z_{sp} is the metallicity sensitivity at 8 Gyr, solar metallicity.

Z_{sp} is surveyed for indices in three photometric systems³. We refer the readers to related papers for detailed description of filters and indices (See §1). As shown in Worthey (1994), indices with Z_{sp} close to 1.5 are less likely to break the age-metallicity degeneracy. Hence, indices with extreme Z_{sp} values are selected as candidates and listed in Table 1⁴. What is not quantified in Table 1 is the dynamic range (compared to observational error) of a given index, and the dynamic range is low in DDO C(41-42), alas.

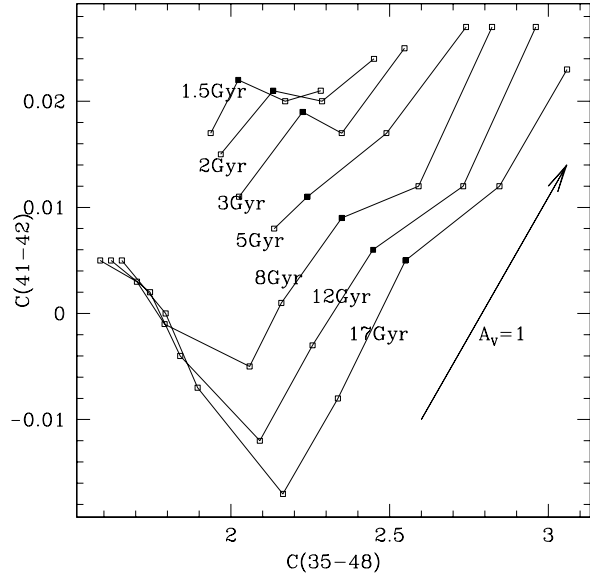


Figure 1. DDO C(35-48) vs. C(41-42) plot. SSPs of the same age are connected as isochrones. Our models (W94) are given at age= 1.5, 2, 3, 5 with $\log(Z) = -0.225, 0, 0.25, 0.50$, and age= 8, 12, 17 Gyr with $\log(Z) = -2.0, -1.5, -1.0, -0.50, -0.25, 0, 0.25, 0.50$. Solar metallicity SSPs are marked as *filled squares* to guide the eye. A vector for $A_V = 1.0$ mag is sketched to estimate the extinction effect.

- DDO system

The extremely low Z_{sp} value of C(41-42) colour makes it a promising age indicator to break the degeneracy. Figure 1 shows C(35-38) vs. C(41-42) plot of our models using W94 stellar evolution. The isochrones are well separated, except SSPs with very low metallicities. However, the major problem is small dynamic range (≈ 0.05 mag) of C(41-42). A little observational error or dust content ($A_V = 1.0$ mag is sketched in Figure 1 to estimate the extinction effect) will destroy the well spaced isochrones. The short distance between the central wavelengths of DDO 41 and 42 filters (≈ 100 Å) is the reason for this defect.

- BATC system

BATC 6075-6660 and 5795-6075 colours show potential of breaking the degeneracy for their Z_{sp} values. However, Figure 2 does not work out as expected. Though the super-solar metallicity SSP isochrones are separated as indicated by Z_{sp} , the sub-solar metallicity SSP isochrones are still highly degenerate. We note that the 6660 filter contains $H\alpha$, which explains age sensitivity of the 6075-6660 colour. However, we also note that the dynamic range of both colours is small compared to the $A_V = 1.0$ mag extinction vector, and that the 6075-6660 colour only spans 0.06 mag total, which seems small compared to reasonable observational errors. Furthermore, since it is $H\alpha$ that is driving the age sensitivity of this colour, it will be sensitive also to nebular emission, which can easily overwhelm the stellar absorption in many galaxies.

¹ <http://ircamera.as.arizona.edu/nircam/>

² <http://stev.oapd.inaf.it/YZVAR/>

³ <http://astro.wsu.edu/models/isochrones.html>

⁴ Since the K band is suggested to be sensitive to young stellar populations, nonstandard colours relative to the K band, like DDO41-K, BATC6075-K, were also examined. However, no promising index is found.

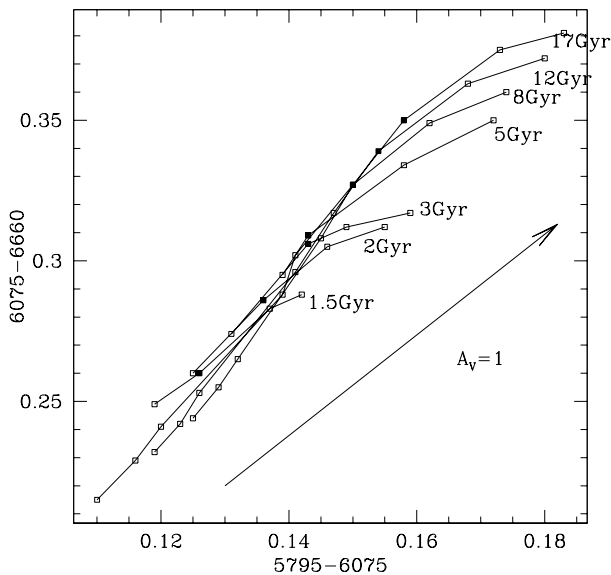


Figure 2. BATC 5795-6075 vs. 6075-6660 plot. Isochrones are described in Figure 1. A vector for $A_V = 1.0$ mag is also sketched to estimate the extinction effect.

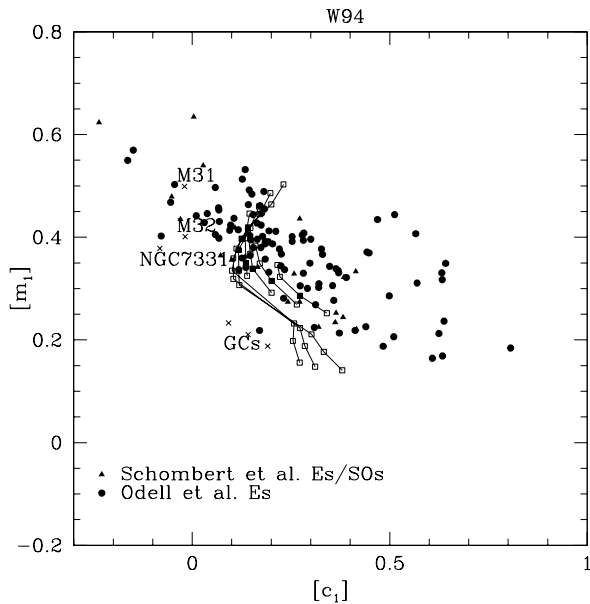


Figure 3. Strömgren c_1 vs. m_1 plot. Isochrones are described in Figure 1. Ages are not labelled for narrow space, but they can be easily inferred from Figure 4. Observables from three samples are labelled with different symbols: *Filled Triangles*: Es and SOs from Schombert et al. (1993). *Crosses*: Nearby Es and GCs from Rakos et al. (1990). *Filled Circles*: Es from Odell et al. (2002).

• Strömgren system

Since $[c_1]$ and $[m_1]^5$ are reddening independent (Strömgren 1966), and they also have promising Z_{sp} values, we take a close look at these two indices. Rakos et al. (1991) suggested

⁵ $c_1 \equiv (u - v) - (v - b)$, $m_1 \equiv (v - b) - (b - y)$;
 $[c_1] \equiv c_1 - 0.2(b - y)$, $[m_1] \equiv m_1 + 0.18(b - y)$.

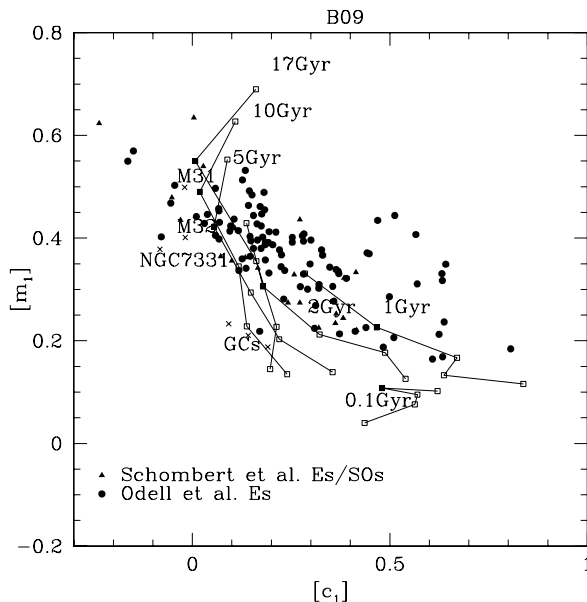


Figure 4. Strömgren c_1 vs. m_1 plot of B09 models. The models are given at age= 0.1, 1, 2, 5, 10, 17 Gyr with $\log(Z) = -2.23, -1.23, -0.53, 0, 0.37$. Solar metallicity SSPs are marked as *filled squares* to guide the eye. Observable symbols are the same as in Figure 3.

m_1 is a metal-line index, while c_1 is a Balmer discontinuity index. Figure 3 confirms $[m_1]$ as a metallicity sensitive index, because the SSP isochrones lie almost parallel to the $[m_1]$ axis. With its reasonable dynamic range (≈ 0.6 mag) and its reddening free advantage, $[c_1]$ vs. $[m_1]$ plot is a promising candidate index that might break the age-metallicity degeneracy. Three samples are selected to test the competency of the $[c_1]$ vs. $[m_1]$ plot: (1) Ellipticals (Es) and SOs from Schombert et al. (1993), shown as *filled Triangles* in Figure 3; (2) Nearby Es and globular clusters (GCs) from Rakos et al. (1990). They are labelled separately for clarity (*crosses*); (3) Es from Odell et al. (2002), shown as *filled circles*. Note that the last two samples are recorded in a modified Strömgren filter system called *uz, vz, bz, yz*. The relations of Rakos et al. (1996) are employed to convert the observables to the *wby* system. Figure 3 shows that our model grids based on W94 evolution do not fit the observations well. B09 model grids are also plotted along the observables in Figure 4. Comparing with Figure 3, the coverage improves greatly in the later model grids, but isochrones of age between 5 and 17 Gyr are still partially degenerate. Obviously, the $[m_1]$ indices of old metal-rich SSPs in B09 models are systematically larger than that in W94 models. We also note that two sets of tracks are not the same, e.g., young age, low metallicity SSPs are not included in W94 models. To investigate the topic furthermore, we draw the $[c_1]$ vs. $[m_1]$ plot of B94 models (§ 2.3), which looks strikingly similar to Figure 4 (not shown in this paper). Thus, the stellar phases causing the dramatic discrepancies between Figure 3 and 4 must be different in W94 and B09 models, but similar in B94 and B09 models. We defer discussion of the specific stellar phases because it is beyond the scope of this work.

Table 2. Index changes at 8 Gyr, solar metallicity

Index	C	N	O	Na	Mg	Fe
DDO C(41-42)	0.028	0.039	-0.018	-0.001	-0.002	-0.001
DDO C(35-48)	0.068	0.026	-0.033	-0.005	-0.002	0.045
BATC 6075-6660	-0.009	-0.006	0.002	0.000	0.001	0.002
BATC 5795-6075	0.005	0.001	-0.004	0.004	-0.001	0.001
Strömgren [m_1]	0.024	0.021	-0.025	-0.003	-0.032	0.029
Strömgren [c_1]	-0.078	-0.015	0.054	0.003	0.080	-0.009

2.2 Element Sensitivity

In a non-solar scaled environment, indices may reflect those abundance changes. To trace the effects of different elements, we increase the stellar atmosphere model abundances of six major elements (C, N, O, Na, Mg, Fe) by 0.3 dex⁶, one single element at a time. The sensitivity is modeled only in the stellar library; the isochrones are kept as published. Table 2 outlines the index changes at 8 Gyr, solar metallicity.

- The prominent carbon and nitrogen effect on DDO C(41-42) colour is not surprising, since the DDO 41 band overlaps CN₁ and CN₂ Lick indices in wavelength. Fe and CN absorption lines are the main features under 4000 Å, which explains the DDO C(35-48) colour changes at super-solar C, N, and Fe abundances. The behavior of increased O is opposite due to molecular balancing: The CO molecule has the strongest binding energy and so adding O decreases the C supply, weakening C₂ and CN features. Thus, adding more O causes bluer DDO C(41-42) and C(35-38) colours.

- The BATC 6075-6660 and 5795-6075 colours are relatively unaffected by six major elements, which makes them good colours to study systems with unknown element enhancements. What we find matches the basic philosophy of creating this photometric system: avoiding known bright feature lines and sky lines, in order to study the continuum of the spectrum (Fan et al. 1996).

- Strömgren [m_1] and [c_1] are different from the four colours above, because they are the subtractions of two colours. [m_1] is found to be metallicity sensitive in § 2.1, which is consistent with its behavior in Table 2: Five elements have substantial influences on [m_1]. The trend of the [c_1] index change due to C and O abundance variations is reverse compared to other indices. Since u and v bands are both blanketed by CN absorption lines, our models predict that the impact of CN on the v band is greater than that on the u band. Therefore, higher CN abundance means a larger magnitude increase in the v band than that in the u band, leading to a smaller [c_1] value. The strong Mg effect on [c_1] is echoed by the Mg3835 (u band) and Mg4780 (b band) indices defined in Serven et al. (2005).

2.3 ($B - V$) vs. ($V - K$) Plots

The possibility of breaking age-metallicity degeneracy with optical plus near-IR colours (de Jong 1996; James et al. 2006; Pessev et al. 2008), and the upcoming era of near-IR telescopes (eg: *JWST*) inspire us to delve the optical near-IR colour-colour plot. Prior to this work, Lee et al.

(2007) inspected the ($B - V$) vs. ($V - K$) plot using Bruzual & Charlot (2003, hereafter BC03), Maraston (2005), and BaSTI (Cordier et al. 2007) models. They suggested different treatments of convective core overshooting and differences in the TP-AGB phase cause the inconsistency among different model grids (also see Maraston et al. 2006). To further discuss the robustness of the models, we investigate the isochrones that looked so promising (B94) and a later, even more complete version (B09) from the same group.

• B94 models

Perhaps partly because of the inclusion of all stellar evolutionary phases, B94 models were widely adopted as basic stellar evolution isochrones for evolutionary synthesis models, such as: BC03; PEGASE (Fioc & Rocca-Volmerange 1997, 1999); and STARBURST99 (Vazquez & Leitherer 2005) models. Figure 5 shows the ($B - V$) vs. ($V - K$) plot of B94 models. Three observational samples are selected for comparison: (1) old, metal-poor GCs from Burstein et al. (1984) (*filled circles*); (2) old, metal-rich Es from Peletier (1989) (*filled triangles*); (3) SWB⁷ type IV–VI Large Magellanic Cloud (LMC) star clusters (*crosses*). The reddening-corrected ($B - V$) and ($V - K$) colours come from Van den Bergh (1981) and Persson et al. (1983). The last sample is selected as “intermediate age” SSPs, roughly 1 to 8 Gyr according to Persson et al. (1983). Generally speaking, observables of these three samples locate at expected locations on the model grids.

• B09 models

With improved understanding of TP-AGB phase, Padova group updated the stellar evolution models. Compared with previous models of this group (B94; Girardi et al. 2000), B09 models adopted a sophisticated TP-AGB model which includes third dredge-up, hot bottom burning, and variable molecular opacities (Marigo et al. 2008). Also, basic observables of AGB stars in the Magellanic Clouds (MCs) were reproduced by the new models (Girardi & Marigo 2007). The ($B - V$) vs. ($V - K$) plot of the B09 models are shown in Figure 6. Observables are also plotted as in Figure 5. Isochrones of age larger than 5 Gyr are consistent with that of the B94 models. Es and GCs locate on the metal-rich and metal-poor sides, respectively. However, isochrones of 1 and 2 Gyr change substantially: the ($V - K$) colour of $\log(Z) = -0.53$ becomes redder than that of solar metallicity. An unreported “S” shape is found if $\log(Z) = -0.53$ SSPs are connected. Another unexpected change is about the isochrone of the youngest age, 100 Myr: the ($V - K$) colour of the lowest metallicity ($\log(Z) = -2.23$) is even redder than that of the highest metallicity ($\log(Z) = 0.37$).

3 DISCUSSION

3.1 Strömgren System: Empirical Leverage?

Prior to this work, c_1 or m_1 were paired with ($u - v$), ($b - y$), or other colours to estimate galaxy age (Russell & Bessell 1989; Rakos et al. 1996). In this paper, the extinction independent Q-indices [c_1] and [m_1] are assembled, but do a

⁶ 0.15 dex for C, to avoid the danger of turning to a carbon star (Serven et al. 2005).

⁷ Searle et al. (1980)

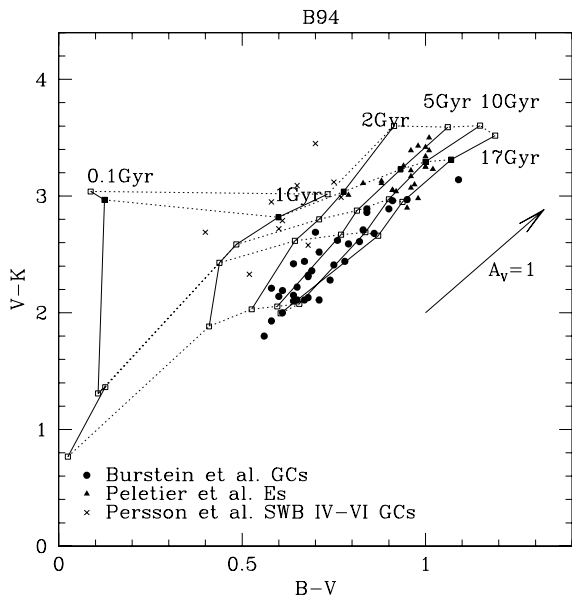


Figure 5. $(B - V)$ vs. $(V - K)$ plot of B94 models. The models are given at age= 0.1, 1, 2, 5, 10, 17 Gyr with $\log(Z) = -1.7, -0.7, -0.4, 0, 0.4$. Solar metallicity SSPs are marked as *filled squares* to guide the eye. SSPs of the same age are connected by *solid lines*, while SSPs of the same metallicity are connected by *dotted lines*. A vector for $A_V = 1.0$ mag is sketched to estimate the extinction effect. Observables from three samples are labelled by different symbols: *Filled Triangles*: Es from Peletier (1989). *Filled Circles*: GCs from Burstein et al. (1984). *Crosses*: SWB type IV–VI Large Magellanic Cloud star clusters from Van den Bergh (1981) and Persson et al. (1983).

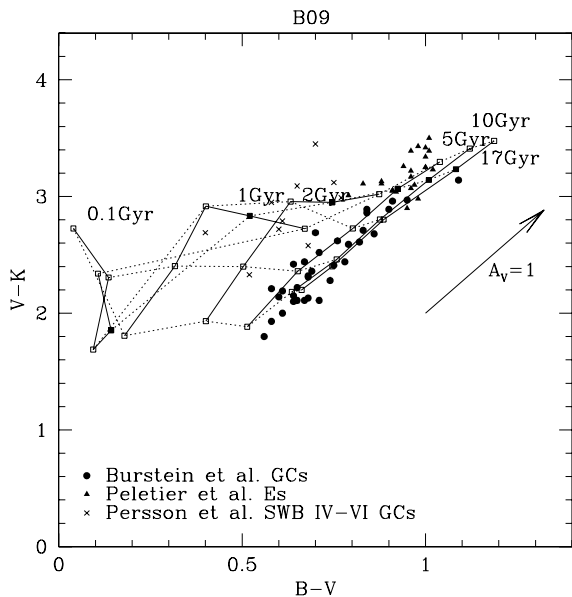


Figure 6. $(B - V)$ vs. $(V - K)$ plot of B09 models. The models are given at age= 0.1, 1, 2, 5, 10, 17 Gyr with $\log(Z) = -2.23, -1.23, -0.53, 0, 0.37$. Other symbols are the same as in Figure 5.

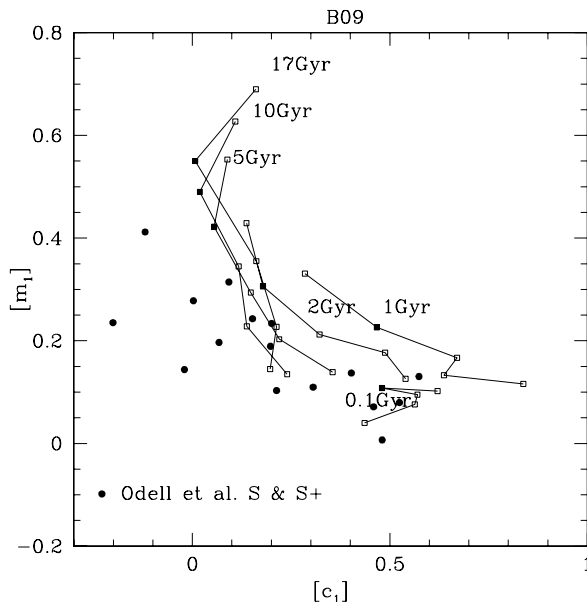


Figure 7. Strömgren $[c_1]$ vs. $[m_1]$ plot of B09 models. The models are described in Figure 4. Solar metallicity SSPs are marked as *filled squares* to guide the eye. *Filled Circles*: S and S+ of Odell et al. (2002).

mediocre job breaking the age-metallicity degeneracy. As seen in Figure 4, several observables lie outside the B09 model grids. Three reasons are hypothesized for these outliers: First, the conversion relations between uz , vz , bz , yz and $uvby$ system presented in Rakos et al. (1996) are empirical, which inevitably increases the uncertainty; Second, the dynamic range of $[c_1]$ index is not large compared to the observational error; Third, isochrones of age between 5 and 17 Gyr are partially degenerate, which reduces the span of model grids.

The model isochrone of 100 Myr lies low in the $[c_1]$ vs. $[m_1]$ plot. This is similar to the statement in Rakos et al. (1996) that most of the starburst galaxies have mz values⁸ less than -0.2 , and they are well separated from other types of galaxies. To test the potential of $[m_1]$ index as a star formation rate indicator, S (“star formation rates equivalent to normal disk galaxy”) and S+ (“starburst objects”) from Odell et al. (2002) are selected and shown in Figure 7. Most of the mz values of this sample are less than -0.1 , supporting the idea that starburst galaxies are bluer in $[m_1]$. However, we detect no clear $[m_1]$ value that separates Es and star forming galaxies.

Strömgren system photometry is far less developed than broad band photometry for galaxies, however. That, plus the large apparent observational scatter in Figures 3, 4 and 7 lead us to conjecture that Strömgren photometry may still have great potential for breaking the age-metallicity degeneracy, but higher quality data are needed to be certain.

⁸ $mz \equiv (vz - bz) - (bz - yz)$

3.2 Model Grid Differences

Three SPS models are assembled in this work: W94, B94, and B09 (i.e., primitive, competent, and sophisticated, respectively.). Figure 3, 4, 5, and 6 clearly illustrate the model differences in $[c_1]$ vs. $[m_1]$ and $(B - V)$ vs. $(V - K)$ plots. During the whole work, we calculate the magnitudes of each bands in three SPS models with the same codes, thus W94, B94, B09 models share the same spectral library, IMF (Salpeter 1955) with lower mass limit $M_{min} = 0.1M_{\odot}$, upper mass limit $M_{max} = 100M_{\odot}$, and etc. Most of the model grid discrepancies rely on different stellar evolution descriptions:

- W94 models are a merging of isochrones and tracks from many sources. Compared to B94, W94 models have a factor of two more stars in the upper RGB. The core-helium burning phase was approximated by a single red clump. The luminosities and lifetimes of AGB stars were drawn from theoretical tracks.

- B94 models included all phases of stellar evolution until the remnant stage in all mass ranges. Convective core overshooting was also considered in the models. Nevertheless, the analytic prescription of TP-AGB phase was approximate. (Marigo et al. 2008)

- B09 models adopted the latest TP-AGB model of Marigo et al. (2008). Compared with previous ones, this TP-AGB model has included several crucial effects and it was calibrated by AGB stars in the MCs. Bertelli et al. reckoned B09 models as satisfactory achievement.

In Figure 6, SSPs with $\log(Z) = -0.53$ have the reddest $(V - K)$ colours along isochrones of 1 and 2 Gyr. This feature is not seen in B94 model grids. Since B94 and B09 models mainly differ in TP-AGB model treatments, which affect the near-IR colour seriously between 0.3 and 2 Gyr (Maraston 2005), it is suggested different treatments of TP-AGB stars are responsible for the changes of model grids. Considering the metallicities of star clusters in the LMC (mean $\log(Z) = -0.42$ for clusters with $1 \leq t < 2$ Gyr and -0.57 for clusters with $2 \leq t < 10$ Gyr, Pessev et al. 2008), SWB IV–VI star clusters are better fitted in B09 models — B94 models give much higher metallicities. Nevertheless, noting that B09 models are calibrated by AGB stars from the MCs, and that the metallicities of star clusters in the LMC are around $\log(Z) = -0.53$, it is suspected that SSPs of other metallicities, especially the extremely low metallicity, may not be well calibrated. The scarcity of very low metallicity AGB stars around solar neighbourhood impedes empirical calibration. It is reasonable to suggest closer scrutiny for SSPs with extremely low metallicities around 1 and 2 Gyr.

Another unexpected feature in Figure 6 is the twist of the 100 Myr isochrone. This youngest isochrone is unique: the $(V - K)$ colour at the lowest metallicity is redder than that of the highest metallicity. This is inconsistent with the usual sense that metal-rich SSPs are redder than metal-poor SSPs (See the 100 Myr isochrone of Figure 5). The change of the 100 Myr isochrones between B94 and B09 models challenge the method of estimating ages and metallicities of young SSPs ($0.1 < t < 1$ Gyr) from optical near-IR colour–colour plots (Brocato et al. 1999; Hunt et al. 2003).

Finally, we check B94 and B09 model differences in the popular $(B - R)$ vs. $(R - K)$ plot (de Jong 1996;

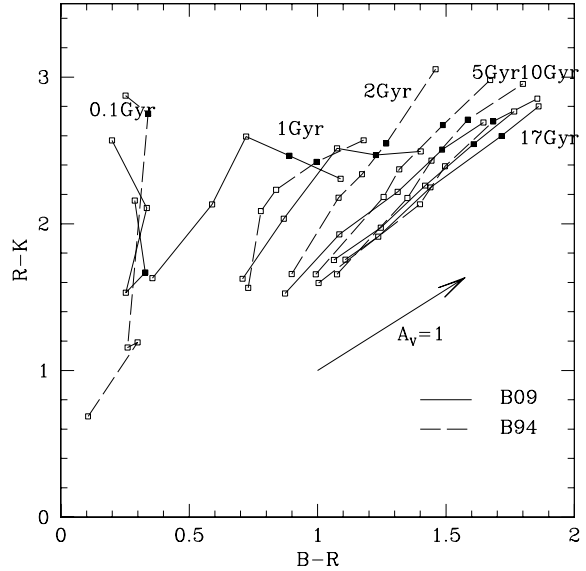


Figure 8. $(B - R)$ vs. $(R - K)$ plot of B94 and B09 models. The B94 models are given at age= 0.1, 1, 2, 5, 10, 17 Gyr with $\log(Z) = -1.7, -0.7, -0.4, 0, 0.4$, while the B09 models are given at age= 0.1, 1, 2, 5, 10, 17 Gyr with $\log(Z) = -2.23, -1.23, -0.53, 0, 0.37$. Note that the two sets of tracks are not identical. Isochrones of B09 models are labelled by *solid lines*, and isochrones of B94 models are labelled by *dashed lines*. Solar metallicity SSPs are marked as *filled squares* to guide the eye. A vector for $A_V = 1.0$ mag is sketched to estimate the extinction effect.

Bell & de Jong 2000, Figure 8). *Solid lines* are isochrones of B09 models; *dashed lines* are isochrones of B94 models. Differences between two model grids are similar to $(B - V)$ vs. $(V - K)$ plots: SSPs of $\log(Z) = -0.53$ have the reddest $(R - K)$ colours along the 1 and 2 Gyr isochrones in B09 models; The $(R - K)$ colour at the lowest metallicity is redder than that at the highest metallicity along the 100 Myr isochrone of B09. Thus, these features are dependent upon near-IR band (K), instead of visible bands (V or R). Considering the TP-AGB treatment differences of B94 and B09 models and the TP-AGB effects on K band, it is again suggested TP-AGB stars are responsible for the changes of young SSP isochrones ($0.1 < t < 2$ Gyr), which is consistent with Maraston et al. (2006) and Lee et al. (2007)

4 SUMMARY

Motivated by the need of estimating ages and metallicities from photometric systems, this work explored the DDO, BATC, Strömgren systems in the hope of finding age sensitive or metallicity sensitive indices. Three index–index plots were examined but only Strömgren $[c_1]$ vs. $[m_1]$ plot showed moderate age-metallicity separation. Four indices of the DDO and Strömgren systems changed substantially while increasing C and N abundances. O traces an opposite trend compared to C and N, since O tends to form CO with C. Then, we turned to the literature-posed age-metallicity disentangling space — the optical plus near-IR colour–colour plot. Updated stellar evolution gives no support for clear disentanglement of age. Even mean age, there-

fore, is a subtle effect in colors, and would require, seemingly, both finer-tuned models and observations of greater accuracy.

REFERENCES

- Baade, W., 1944, *ApJ*, 100, 137
- Bell, E. F., de Jong, R. S., 2000, *MNRAS*, 312, 497
- Bertelli, G., Bressan, A., Chiosi, C., Fagotto, F., Nasi, E., 1994, *A&AS*, 106, 275
- Bertelli, G., Girardi, L., Marigo, P., Nasi, E., 2008, *A&A*, 484, 815
- Bertelli, G., Nasi, E., Girardi, L., Marigo, P., 2009, *A&A*, 508, 355
- Brocato, E., Castellani, V., Raimondo, G., Romaniello, M., 1999, *A&AS*, 136, 65
- Bruzual A., G., Charlot, S., 1993, *ApJ*, 405, 538
- Bruzual A., G., Charlot, S., 2003, *MNRAS*, 344, 1000
- Burstein, D., Faber, S. M., Gaskell, C. M., Krumm, N., 1984, *ApJ*, 287, 586
- Cardiel, N., Gorgas, J., Sanchez-Blazquez, P., Cenarro, A. J., Pedraz, S., Bruzual, G., Klement, J., 2003, *A&A*, 409, 511
- Carter, D. et al., 2009, *MNRAS*, 397, 695
- Charlot, S., Worthey, G., Bressan, A., 1996, *ApJ*, 457, 625
- Conroy, C., Gunn, J. E., White, M., 2009, *ApJ*, 699, 486
- Cordier, D., Pietrinferni, A., Cassisi, S., Salaris, M., 2007, *AJ*, 133, 468
- de Jong, R. S., 1996, *A&A*, 313, 377
- Dotter, A., Chaboyer, B., Jevremovic, D., Kostov, V., Baron, E., Ferguson, J. W., 2008, *ApJS*, 178, 89
- Faber, S. M., Friel, E. D., Burstein, D., Gaskell, C. M., 1985, *ApJS*, 57, 711
- Fan, X. et al., 1996, *AJ*, 112, 628
- Fioc M., Rocca-Volmerange B., 1997, *A&A*, 326, 950
- Fioc M., Rocca-Volmerange B., 1999, preprint (arXiv:astro-ph/9912179)
- Girardi, L., Bressan, A., Bertelli, G., Chiosi, C., 2000, *A&AS*, 141, 371
- Girardi, L., Marigo, P., 2007, *A&A*, 462, 237
- Gorgas, J., Faber, S. M., Burstein, D., Gonzalez, J. J., Courteau, S., Prosser, C., 1993, *ApJS*, 86, 153
- Hunt, L. K., Thuan, T. X., Izotov, Y. I., 2003, *ApJ*, 588, 281
- James, P. A., Salaris, M., Davies, J. I., Phillipps, S., Cassisi, S., 2006, *MNRAS*, 367, 339
- Lee, H., Worthey, G., Trager, S. C., Faber, S. M., 2007, *ApJ*, 664, 215
- Maraston, C., 2005, *MNRAS*, 362, 799
- Maraston, C., Daddi, E., Renzini, A., Cimatti, A., Dickinson, M., Papovich, C., Pasquali, A., Pirzkal, N., 2006, *ApJ*, 652, 85
- Marigo, P., Girardi, L., Bressan, A., Groenewegen, M. A. T., Silva, L., Granato, G. L., 2008, *A&A*, 905, 883
- McClure, R. D., 1976, *AJ*, 81, 182
- McClure, R. D., Van den Bergh, S., 1968, *AJ*, 73, 313
- Odell, A. P., Schombert, J., Rakos, K., 2002, *AJ*, 124, 3061
- Peletier, R. F., 1989, Ph.D. Thesis, Univ. Groningen
- Peletier, R. F., Valentijn, E. A., Jameson, R. F., 1990, *A&A*, 233, 62
- Persson, S., Aaronson, M., Cohen, J., Frogel, J., Matthews, K., 1983, *ApJ*, 266, 105
- Pessev, P. M., Goudfrooij, P., Puzia, T. H., Chandar, R., 2008, *MNRAS*, 385, 1535
- Poole, V., Worthey, G., Lee, H.-C., Serven, J., 2010, *AJ*, 139, 809
- Rakos, K. D., Kreidl, T. J., Schombert, J. M., 1990, *Astrophysics and Space Science*, 170, 239
- Rakos, K. D., Maindl, T. I., Schombert, J. M., 1996, *ApJ*, 466, 122
- Rakos, K. D., Schombert, J. M., Kreidl, T. J., 1991, *ApJ*, 377, 382
- Russell, S. C., Bessell, M. S., 1989, *ApJS*, 70, 865
- Salpeter, E. E., 1955, *ApJ*, 121, 161
- Schombert, J. M., Hanlan, P. C., Barsony, M., Rakos, K. D., 1993, *AJ*, 106, 923
- Searle, L., Wilkinson, A., Bagnuolo, W. G., 1980, *ApJ*, 239, 803
- Serven, J., Worthey, G., Briley, M. M., 2005, *ApJ*, 627, 754
- Serven, J., Worthey, G., Toloba, E., Sanchez-Blazquez, P., 2011, *AJ*, 141, 184
- Shang, Z. et al., 1998, *ApJ*, 504, L23
- Strömgren, B., 1966, *ARA&A*, 4, 433
- Thomas, D., Maraston, C., Bender, R., 2003, *MNRAS*, 339, 897
- Tinsley, B. M., 1968, *ApJ*, 151, 547
- Tinsley, B. M., 1978, *ApJ*, 222, 14
- Van den Bergh, S., 1981, *A&AS*, 46, 79
- Vazquez G. A., Leitherer C., 2005, *ApJ*, 621, 695
- Worthey, G., 1994, *ApJS*, 95, 107
- Worthey, G., Faber, S., Gonzalez, J. J., Burstein, D., 1994, *ApJS*, 94, 687
- Worthey, G., Ottaviani, D. L., 1997, *ApJS*, 111, 37